

On the control of carbon nanostructures for hydrogen storage applications

Patrice Guay^a, Barry L. Stansfield^a, Alain Rochefort^{b,*}

^a INRS—Énergie, Matériaux et Télécommunications, 1650 boulevard Lionel-Boulet C.P. 1020, Varennes, Qué, Canada J3X 1S2

^b Département de génie physique, École Polytechnique de Montréal, C.P. 6079 Succ. Centre-Ville, Montréal, Qué, Canada H3C 3A7

Received 15 October 2003; accepted 23 April 2004

Available online 25 May 2004

Abstract

The storage of hydrogen in different carbon nanostructures has been investigated using classical Monte–Carlo simulations techniques. Very low hydrogen uptakes ($\leq 1\%$ wt) have been calculated for single-walled and double-walled carbon nanotubes, as well as for graphite nanofibers at 293 K and 10 MPa. The amount of hydrogen uptake strongly depends on the porosity within the nanostructure network where optimal arrangements give rise to the formation of a well-defined two-dimensional adsorbed hydrogen layer. The presence of metallic impurities within single-walled nanotube bundles was modeled by disseminating atomic particles, characterized by a highly attractive potential, throughout the nanotube network. It has been found that the presence of metallic particles significantly enhances the hydrogen uptake, but not to a point where this could be considered a promising storage solution.

© 2004 Elsevier Ltd. All rights reserved.

Keywords: A. Carbon nanotubes, Graphite nanofibers, Doped carbon; C. Molecular simulation; D. Gas storage

1. Introduction

Hydrogen storage in carbon nanostructures (CNS) remains a controversial topic because early work that showed very promising storage capacity in single-walled carbon nanotubes (SWNTs) and graphite nanofibers (GNFs) has not been clearly reproduced [1–4]. For example, high hydrogen uptakes from 4.2% to 65% wt have been reported for SWNTs and GNFs at 300 K under around 10 MPa [2,4]. This strongly contrasts with the low hydrogen uptakes ($\leq 1\%$ wt) claimed in other recent experimental works [5–7]. On the other hand, most of the theoretical and numerical studies agree, predicting a relatively low storage capacity in purified carbon nanostructures (SWNTs, GNFs) at room temperature [8–12]. In addition, recent experimental work on hydrogen adsorption has clearly demonstrated the influence of metallic impurities on the final hydrogen uptake [13]. For example, titanium alloy particles originating from the degradation of the probe during a

sonication treatment of SWNT samples increase the amount of adsorbed hydrogen to about 1.47% wt when the titanium loading is 59.6% wt. Therefore, it clearly appears that the amount of stored hydrogen gas in a purified sample would be much lower than the 2010 DOE target of 6.0% wt [14].

Other metallic impurities or particles such as Fe, Ni and Co could originate from the residual catalyst used during carbon nanostructure synthesis. Even very sophisticated purification techniques can only reduce their amount to approximately 1–2% wt. Similarly to supported metal particles, the existence of metallic atoms, clusters or particles within a carbon nanostructure network can significantly modify the apparent amount of adsorbed hydrogen [15]. The hydrogen adsorption into CNS can occur through several mechanisms, such as chemisorption on metallic particles [16], dissociative adsorption on metal followed by atomic hydrogen spillover into the CNS matrix [17,18], or through a direct dissolution of hydrogen into the metallic particles to form a hydride phase [19]. Following these last possible pathways, activated processes could take place during adsorption, and finally lead to a rather complex desorption spectrum where different

* Corresponding author. Tel.: +1-514-340-4711; fax: +1-514-340-3218.

E-mail address: alain.rochefort@polymtl.ca (A. Rochefort).

hydrogen phases could be observed. Although a careful theoretical and experimental investigation of the different possible mechanisms would be necessary, the effect of impurities in a CNS network on the adsorption capacity first needs to be addressed.

In this study, the adsorption of hydrogen in several different CNS (SWNTs, double-walled nanotubes (DWNTs) and GNFs) has been examined as a function of the van der Waals gap or distance between the cylindrical walls in the case of tubes or between the sheets in the case of fibers. The influence of disseminated metallic particles within a CNS network on the final hydrogen storage adsorption has also been addressed. Although the approximation considered in the description of the potential energy between hydrogen and metallic impurities was crude, the significant variation observed in the amount of adsorbed hydrogen is discussed in terms of the possible storage capacity of metallic-doped carbon nanostructures as reservoirs for hydrogen.

2. Computational details

Grand canonical Monte–Carlo (GCMC) simulations of hydrogen adsorption at room temperature (293 K) and moderate pressure (10 MPa) were carried out with a modified version of the *BigMac* package [20–22]. This GCMC software was adapted to study H_2 /CNS models, and to include quadrupolar interactions in the evaluation of the total potential energy. During the simulations, the events of creation, destruction or displacement of hydrogen in configurational space were equiprobable (33%). A typical simulation performed 10^6 steps to ensure that an equilibrium configuration was reached, followed by 2×10^6 steps to evaluate the number of hydrogen molecules (N_{H_2}) in the volume considered.

The standard unit cell, where periodic boundary conditions were applied, is shown in Fig. 1, where we also identify the intra- and intertubular adsorption sites. For the $(n, 0)$ SWNT and DWNT models considered, the most stable hexagonal arrangement of nanotubes within a bundle [23] was used. The amount of adsorbed hydrogen was computed as a function of two structural parameters: the nanotube diameter (D_{NT}) and the van der Waals (vdW) gap. Due to the boundary conditions, we have mostly considered hydrogen adsorption in periodic arrays of nanotubes. The amount of hydrogen adsorbed on the outer surface of a hypothetical finite nanotube bundle was not explicitly evaluated, but rather estimated for a few cases from the variation of hydrogen density with the vdW gap. The structural parameters and the C–C bond distance (1.42 Å) of the CNS model were kept fixed during GCMC runs, and the interaction energy between carbon atoms was not evaluated explicitly. The sum of the interaction energies between N

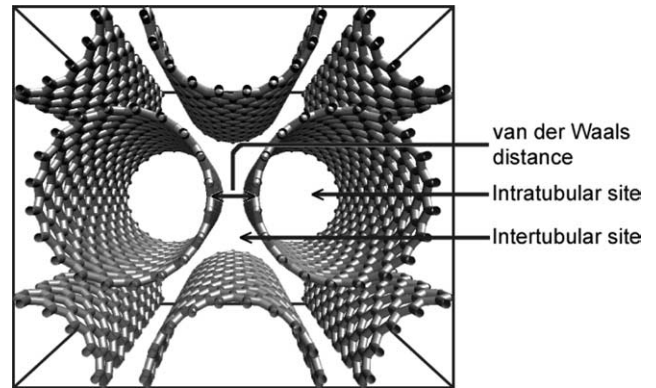


Fig. 1. A typical unit cell containing a hexagonal arrangement of $(20,0)$ SWNTs, where tri-dimensional periodic boundary conditions were applied. The different adsorption sites in the SWNT rope, as well as the van der Waals distance (gap), are also identified.

hydrogen molecules and the M carbon atoms in the CNS models is estimated with the classical 6–12 Lennard–Jones (L–J) potential (see Eq. (1)), where r_{ij} is the distance between the centre of mass of the different molecules and k_B is Boltzmann’s constant.

$$U_{H_2-X} = 4k_B\epsilon_{H_2-X} \sum_{i=1}^N \sum_{j=1}^M W(r_{ij}) \left[\left(\frac{\sigma_{H_2-X}}{r_{ij}} \right)^{12} - \left(\frac{\sigma_{H_2-X}}{r_{ij}} \right)^6 \right] + \text{quadrupole interactions} \quad (1)$$

A similar equation was used for H_2 – H_2 interaction except that the second summation was performed over $j = i + 1$ to M in order to avoid double counting. The parameters of the L–J potential, $\epsilon_{H_2-X} = 28.2$ K (36.7 K) and $\sigma_{H_2-X} = 0.3400$ nm (0.2958 nm) used for $X = C$ (H_2), are similar to parameters used in previous studies [8–10]. The cutoff function ($W(r_{ij})$) limits the evaluation of the potential energy between particles i and j to a critical radius fixed at 1.538 nm. In order to simulate the chemisorption of hydrogen on the metallic particles, a highly attractive and localized L–J potential, taking $\epsilon_{H_2-metal} = 2820$ K and $\sigma_{H_2-metal} = 0.1700$ nm, was used. Although the use of a more complex potential for this H_2 –metal interaction would allow a more rigorous description of the chemisorption process, this approximate potential should be sufficient to qualitatively evaluate the effect of metallic particles such as atoms or small clusters disseminated in the CNS network.

The gravimetric (ρ_w) and volumetric (ρ_v) densities of hydrogen were calculated using Eqs. (2) and (3), respectively. N_{H_2} , N_C and N_{metal} are the number of hydrogen molecules, carbon atoms and impurity particles in the unit cell of volume V . Molar masses m_{H_2} and m_C are respectively equal to 2.0 and 12.0 g/mol. We arbitrarily fixed m_{metal} at 58.7 g/mol, the molar mass of nickel. N_A is Avogadro’s constant.

$$\rho_w = \frac{N_{H_2} m_{H_2}}{N_{H_2} m_{H_2} + N_C m_C + N_{metal} m_{metal}} \times 100\% \text{ wt} \quad (2)$$

$$\rho_v = \frac{N_{H_2} m_{H_2}}{N_A V} \times \frac{1 \text{ kg}}{1000 \text{ g}} \quad (3)$$

3. Results and discussion

3.1. Adsorption in pure CNS

In this section, we compare the storage capacity of SWNTs, DWNTs and GNFs ($T = 293 \text{ K}$, $P = 10 \text{ MPa}$) as a function of the porosity. For simplicity, we associate the porosity to the vdW gap, which is the interplanar distance between the nanotubes or graphene sheets. Fig. 2 shows the gravimetric and volumetric amount of adsorbed hydrogen in SWNTs, DWNTs and GNFs as a function of the van der Waals gap, and Fig. 3 illustrates the distribution of hydrogen within the carbon network. Each snapshot of Fig. 3 represents the configuration of hydrogen at the end of a numerical simulation. In a general manner, the amount of adsorbed hydrogen in all carbon nanostructures remains

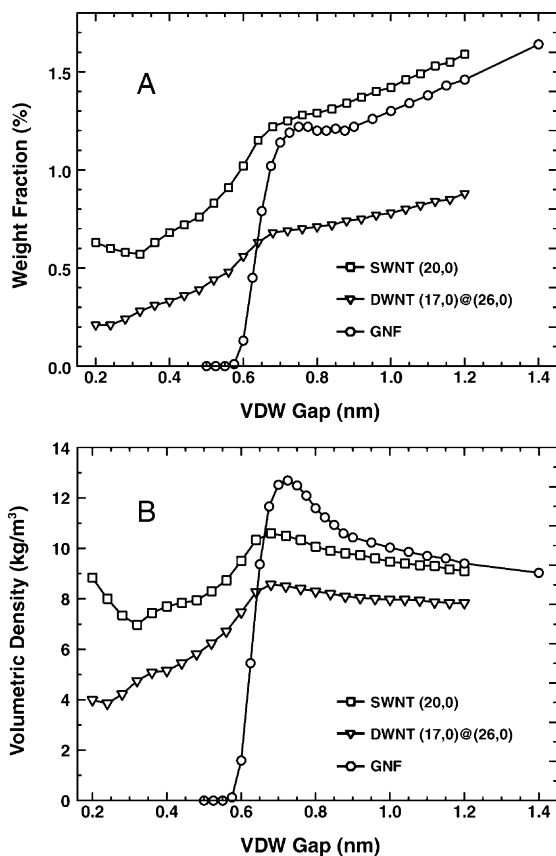


Fig. 2. Gravimetric (A) and volumetric (B) density of hydrogen in SWNT: (20,0), DWNT: (17,0)@(26,0) and GNF as a function of the porosity. Simulations were performed at $T = 293 \text{ K}$ and $P = 10 \text{ MPa}$.

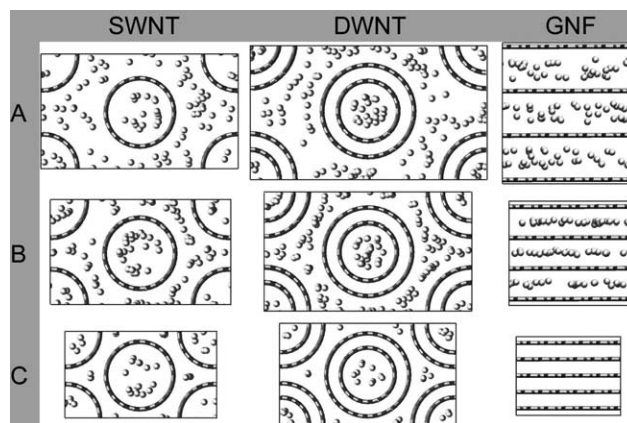


Fig. 3. Snapshots of adsorbed hydrogen in single-walled nanotubes (SWNT), double-walled nanotubes (DWNT), and graphite nanofibers (GNF), for vdW gap of (A) 1.0 nm, (B) 0.7 nm and (C) 0.4 nm.

relatively small for the porosity considered and is smaller than 0.6% wt (7.1 kg/m^3) for nanostructures in which the vdW gap is similar to the bulk interplanar distance in graphite, i.e., 0.3355 nm.

The curves for SWNTs show three distinct regimes between 0.2 and 1.2 nm. Below 0.3 nm, hydrogen is mostly located within the tubes, a small amount is located directly in the interstice between three tubes (3-fold interstice), and there is practically none in the porosity between two tubes (2-fold interstice) due to the small spacing (see also Fig. 3C). From 0.3 to 0.7 nm, the amount of hydrogen increases significantly. At 0.34 nm, it would correspond to the usual structure found for SWNT bundles [23], in which case the computed hydrogen density is 0.60% wt (7.1 kg/m^3). A local maximum of the density can be distinguished around 0.7 nm, and corresponds to the optimal distance for adsorbing a single quasi-2D layer of hydrogen around each nanotube. This quasi-2D structure of adsorbed H_2 monolayer can be clearly observed in Fig. 3B for the three CNS considered. For a vdW gap between 0.7 and 1.2 nm, the gravimetric density of hydrogen increases almost linearly with the vdW gap, or in other words, with the total volume of the reservoir, but the volumetric density is gradually decreasing. These last trends are not really surprising; we can expect the N_{H_2}/N_C ratio (where N_C is constant) to increase with the reservoir volume, and the volumetric density to approximately converge to the compressed hydrogen value, i.e., 7.4 kg/m^3 , for very large vdW gaps. In addition, Fig. 3A shows that hydrogen is randomly distributed throughout the available CNS structure with large vdW gaps.

It is interesting to note that SWNTs show their lowest storage capacity for a vdW gap around 0.34 nm, i.e., at the bulk graphite distance, and that the volumetric density of hydrogen (7.1 kg/m^3) is even lower than for compressed hydrogen (7.4 kg/m^3). This observation is a direct consequence of the boundary conditions used in

which we have not explicitly considered hydrogen adsorption on the outer surface of finite nanotube bundles. This is particularly crucial for systems with a small vdW gap. For bundles with a large vdW gap, the entire surface of the individual nanotubes is accessible, and represents the upper limit of the adsorption capacity of a bundle. As shown by Williams and Eklund, a maximal hydrogen gravimetric density ($<1.5\%$ wt at 300 K and 10 MPa) can be reached with a bundle made of individual nanotubes [12]. We found a similar hydrogen density for an array of nanotube with a vdW gap around 0.7 nm, and for which the entire outer surface is accessible to hydrogen. From this result, we can roughly estimate the contribution of the outer surface of a finite bundle to the amount of adsorbed hydrogen. For example, if we consider that half of the surface of nanotubes in the outer region of a bundle with vdW gap of 0.34 nm are participating in hydrogen adsorption, then the gravimetric hydrogen density should increase from 0.55% wt for a periodic array of nanotubes (see Fig. 2A) to 0.85% wt and 0.67% wt for bundles made of 7 and 91 nanotubes, respectively. Obviously, the variation in hydrogen density between a periodic array and a finite bundle becomes smaller as the number of nanotubes in the bundle increases.

A similar picture of adsorption curves can be derived for DWNTs but here the weight fraction is approximately a factor of 2 lower due to the presence of two nanotube walls. First, we notice in Fig. 3 that no hydrogen adsorbs between the two walls of a single DWNT because of the small spacing (0.3355 nm) between them. Due to the presence of this dead volume in DWNTs, the amount of adsorbed hydrogen remains below the compressed hydrogen value of 7.4 kg/m^3 over a large range of vdW gaps. A maximal value of 8.6 kg/m^3 is reached for a vdW gap of 0.7 nm. Nevertheless, although this illustrates the low storage capacity of DWNTs, an interesting structural effect associated to the presence of two walls can be noted. This effect already occurs for SWNTs, where the density of hydrogen increases when the vdW gap is decreased from 0.35 to 0.20 nm (see Fig. 2A and B), i.e., where hydrogen is essentially located in the intratubular region. This increasing amount of hydrogen is partly related to the presence of an additional attractive potential energy produced by the next nanotube wall, and leads to a combination of the two L–J potentials in which the hydrogen–carbon interaction is slightly more attractive. Consequently, hydrogen appears more strongly bonded.

For DWNTs, this structural effect mainly occurs for an increasing porosity where the variation in the amount of adsorbed hydrogen for a (17,0)@(26,0) DWNT is more important ($+3.5 \text{ kg/m}^3$) than for a (25,0) SWNT ($+2.33 \text{ kg/m}^3$) when the vdW gap is increased from 0.33 to 0.70 nm. A comparison of the hydrogen configurations in SWNTs and DWNTs at a large porosity shown

in Fig. 3A and B clearly demonstrates the consequence of this structural effect. Finally, if we extend these results for DWNTs to the case of multi-walled nanotubes (MWNTs) where the dead volume between nanotube walls is much more important, the volumetric and gravimetric densities of adsorbed hydrogen in MWNTs would be very small. This result strongly contrasts with previous works on MWNTs in which the gravimetric hydrogen density varies from 0.25% wt at 300 K and 0.1 MPa [25], to 5% wt at 300 K and 10 MPa [26].

The results obtained for GNFs clearly show the importance of porosity on hydrogen adsorption and reinforce our interpretation of the adsorption of hydrogen within nanotubes. For GNFs with a vdW gap smaller than 0.6 nm, no hydrogen adsorption appears feasible. Nevertheless, in this range, SWNTs and DWNTs show significant amounts of adsorbed hydrogen located mainly within the nanotubes, with a small fraction located in the porosity due to 3-fold interstices created from the packing of the cylindrically shaped nanotubes. From 0.6 to 0.7 nm, the amounts of adsorbed hydrogen in GNFs increases sharply to a maximum similar to the case of SWNTs, with the maximum corresponding to a single quasi-2D layer of adsorbed hydrogen (see Fig. 3B). For larger porosity, the gravimetric amount of hydrogen increases linearly with the porosity as observed for SWNTs, and its volumetric density slowly converges to the compressed hydrogen value of 7.4 kg/m^3 . From these results, hydrogen adsorption within graphite sheets or carbon nanofibers does not seem an interesting possibility, except if one could significantly expand the graphite interplanar distance by a factor of around 100%, i.e., from 0.34 to 0.70 nm.

These results suggest that carbon nanostructures do not appear to be very interesting candidates for use as hydrogen storage reservoirs. Even the possibility of significantly improving the porosity of the systems, which would be experimentally very difficult, does not increase the amount of adsorbed hydrogen to a level adequate for practical hydrogen storage.

3.2. Influence of metallic particles

Although most of the samples used in hydrogen adsorption experiments are purified through drastic chemical means, these pretreatments are always insufficient to remove the entire amount of transition metals originating from the catalyst used for the synthesis of the carbon nanostructures [24]. In addition, the transition metal left after purification can be found in various forms such as atoms, clusters or nanoparticles which would react differently with molecular hydrogen. However, the modeling of the interaction of hydrogen with transition metals constitutes a tremendous and challenging task, especially in the context of Monte–Carlo

simulations where many different configurations would have to be considered. Several mechanisms such as molecular adsorption, dissociative adsorption, diffusion and desorption can occur [18,28], and have to be taken into account for an accurate description of the interaction. Even if we reduce the number of possible mechanisms to a strict minimum, i.e., only molecular chemisorption on metallic atoms is taken into account, we can still obtain valuable information on the effect of metal on the amount of adsorbed hydrogen.

In our models, a random dispersion [30] of metal atoms within the structure made up of 3-fold interstices in a SWNT network was used. The metal–hydrogen interaction is described by a highly attractive L–J potential ($\epsilon_{\text{H}_2\text{-metal}} = 2820$ K, $\sigma_{\text{H}_2\text{-metal}} = 0.1700$ nm) where ϵ and σ were approximated from experimental data for hydrogen chemisorbed on Fe, Ni and Co [31]. The ratio between impurity and carbon atoms was kept constant at $N_{\text{imp}}/N_{\text{C}} = 1/480$ which would roughly correspond to a 1.0% wt content of nickel impurities. Although large particles would preferably sit on the outer surface of the carbon nanotube ensemble, the presence of atomic particles within the network constitutes a possible distribution that is reminiscent of intercalated graphite materials [29].

Fig. 4 shows the gravimetric (A) and volumetric (B) density of adsorbed hydrogen as a function of the vdW gap for systems of both pure SWNTs and SWNT + impurities. Fig. 5 compares different views of the hydrogen distribution within systems of SWNT + impurities for vdW gap of 1.0 (A), 0.7 (B) and 0.4 nm (C). The presence of impurities in Fig. 5 is clearly identified by the dark spheres within the 3-fold interstices of the SWNT network. As observed for pure SWNTs with intertube distances below 0.30 nm, hydrogen mainly fills the intratubular porosity, with a small amount located in the 3-fold interstices. At this stage, the impurities are not playing a significant role, but even though the available 3-fold volume is small, a few hydrogen molecules are bonded to metallic particles. For vdW gaps between 0.30 and 0.70 nm, the hydrogen density increases quite rapidly, in a similar fashion for both pure and metal-doped SWNTs. Nevertheless, the presence of impurities induces an additional 10% of adsorbed hydrogen for a vdW gap of 0.72 nm which corresponds to a volumetric density increase from 10.6 to 11.7 kg/m³. This increase occurs at a fairly small vdW gap; once the hydrogen is not energetically restricted to occupy the centre of the 3-fold interstices, the impurities become rapidly saturated with hydrogen and their contribution to the total amount of adsorbed hydrogen become constant. For vdW gaps larger than 0.72 nm, the variation in the volumetric density is very similar for both systems.

In addition, we have found a linear dependence between the amount of adsorbed hydrogen and the impurity content that allows us to estimate that an

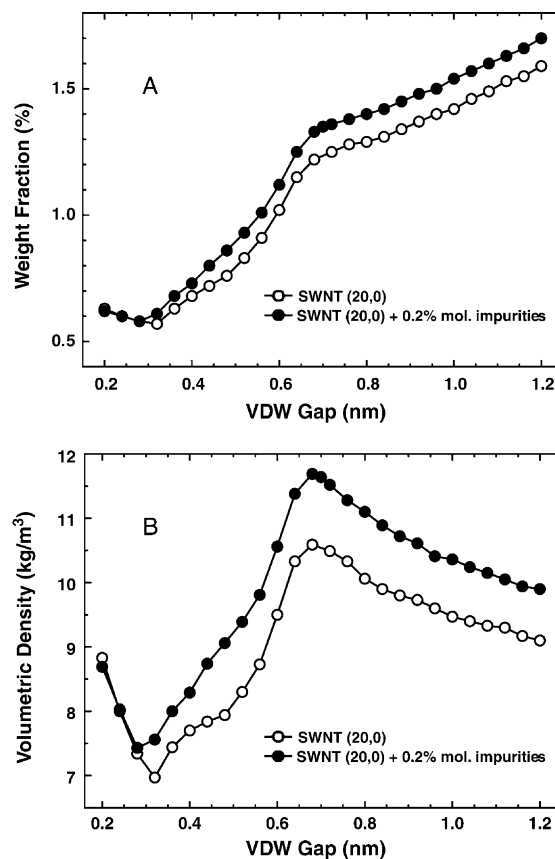


Fig. 4. Gravimetric (A) and volumetric (B) density of hydrogen in SWNT containing impurities as a function of the porosity. Simulations were performed at $T = 293$ K, $P = 10$ MPa.

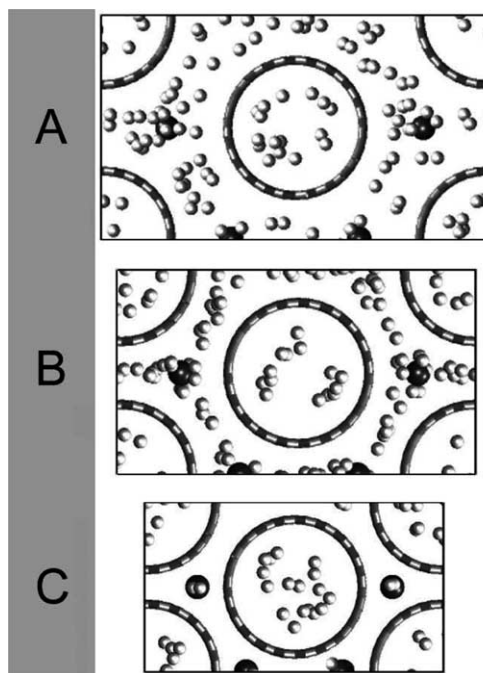


Fig. 5. Snapshots of adsorbed hydrogen in SWNT containing metallic impurities for porosity (A) 1.0 nm, (B) 0.7 nm and (C) 0.4 nm.

impurity content of around 45% wt in a (20,0) sample with a vdW gap of 0.72 nm would be necessary to reach the target fixed by the DOE. In this case, hydrogen adsorption would occur essentially on the “impurities”, with the SWNTs simply playing the role of a supporting matrix. It should be mentioned that we considered the presence of atomic-like particles which are totally accessible to hydrogen and can chemisorb up to around three (3) hydrogen molecules. In reality, the size of the metallic particles could be much larger, and the metallic atoms are thus not totally accessible to chemisorb hydrogen since most of them are within the bulk of the particles.

Hirscher et al. [13] have shown that a sample containing as much as 60% wt of a titanium alloy with particle sizes up to 1 μm increases the hydrogen gravimetric density to only about 1.47% wt. Furthermore, since the maximum storage capacity of pure Ti is 4% wt [32], corresponding to a TiH_2 hydride phase, it is clear that the DOE target cannot be reached easily at room temperature under a moderate pressure (10 MPa) by simply increasing the titanium alloy content. Our results are in agreement with this last observation and other similar studies [18]; reasonable volumetric density of hydrogen (in kg/m^3) can be reached, but only with high metal loading. In contrast, the high atomic weight of transition metals would significantly lower the hydrogen gravimetric density (in% wt) with respect to the DOE target (6.0% wt). A possibly interesting alternative material for hydrogen storage could possibly be obtained by dispersing promising small metal–hydride [33] particles (LaNi_5 , MgNi) in these porous CNS materials. This would allow an increase of the exposed surface area of the metal–hydride, thus creating an additional source of potential hydrogen adsorption sites.

4. Conclusions

Hydrogen uptake in different carbon nanostructures at 10 MPa and 293 K using grand canonical Monte–Carlo numerical simulations have been calculated. Our results indicate that hydrogen adsorption is strongly influenced by the structure porosity. A maximum hydrogen uptake is computed for a porosity of around 0.70 nm, which corresponds to the formation of 2D-like layer of adsorbed hydrogen. However, our simulations indicate that pure carbon nanostructures could not reach a hydrogen uptake of 6.0% wt. The amount of adsorbed hydrogen in SWNTs, DWNTs (MWNTs) and GNFs is lower than 1.4% wt for the optimum porosity around 0.70 nm. For standard carbon nanostructures in which the porosity is similar to the bulk interplanar distance in graphite (0.34 nm), the amount of adsorbed hydrogen is lower than 0.6% wt. The presence of metallic impurities in a SWNT network would improve

the hydrogen adsorption capacity of CNS but it still remains far below the DOE target.

Acknowledgements

Support for this work was provided by the National Sciences and Engineering Research Council of Canada (NSERC). We also acknowledge the Réseau Québécois de Calcul Haute Performance (RQCHP) for providing computational facilities.

References

- [1] Dillon AC, Jones KM, Bekkedahl TA, Klang CH, Bethune DS, Heben MJ. *Nature* 1997;386:377.
- [2] Chambers A, Park C, Baker RTK, Rodriguez NM. *J Phys Chem B* 1998;102:4253.
- [3] Ye Y, Ahn CC, Witham C, Fultz B, Liu J, Rinzler AG, et al. *Appl Phys Lett* 1999;74:2307.
- [4] Liu C, Fan YY, Liu M, Cong HT, Cheng HM, Dresselhaus MS. *Science* 1999;286:1127.
- [5] Ahn CC, Ye Y, Ratnakumar BV, Witham C, Bowman Jr RC, Fultz B. *Appl Phys Lett* 1998;73:3378.
- [6] Tibbetts GG, Meisner GP, Olk CH. *Carbon* 2001;39:2291.
- [7] Hirscher M, Becher M, Haluska M, Quintel A, Skakalova V, Choi Y-M, et al. *J Alloys Compd* 2002;330–332:654.
- [8] Darkrim F, Levesque D. *J Chem Phys* 1998;109:4981.
- [9] Rzepka M, Lamp R, de la Casa-Lillo MA. *J Phys Chem B* 1998;102:10894.
- [10] Wang Q, Johnson JK. *J Phys Chem B* 1999;103:277.
- [11] Wang Q, Johnson JK. *J Chem Phys* 1999;110:577.
- [12] Williams KA, Eklund PC. *Chem Phys Lett* 2000;320:352.
- [13] Hirscher M, Becher M, Haluska M, Dettlaff-Weglikowska U, Quintel A, Duesberg GS, et al. *Appl Phys A* 2001;72:129.
- [14] DOE targets are 4.5% wt by 2005, 6.0% wt by 2010, and 9.0% by 2015. Source: <http://www.eere.energy.gov/hydrogenandfuelcells/>.
- [15] Miller JT, Meyers BL, Barr MK, Modica FS, Koningsberger DC. *J Catal* 1996;159:41.
- [16] Christmann K. *Prog Surf Sci* 1995;48:15, and references therein.
- [17] Teichner SJ. In: Inui T, Fujimoto K, Uchijima T, Masai M, editors, *New Aspects of Spillover Effect in Catalysis*, *Stud in Surf Sci and Catal*, vol. 77, Amsterdam: Elsevier; p. 25.
- [18] Ozaki J, Ohizumi W, Oya A, Illan-Gomez MJ, Roman-Martinez MC, Linares-Solano A. *Carbon* 2000;38:775.
- [19] Wipf H, editor. *Hydrogen in Metals III*. Berlin: Springer; 1997.
- [20] Smit B, Siepmann JI. *J Phys Chem* 1994;98:8442.
- [21] Smit B, Karaborni S, Siepmann JI. *J Chem Phys* 1995;102:2126.
- [22] Vlugt TJH, Krishna R, Smit B. *J Phys Chem B* 1999;103:1102.
- [23] Thess A, Lee R, Nikolaev P, Dai H, Petit P, Robert J, et al. *Science* 1996;273:483.
- [24] Chiang IW, Brinson BE, Smalley RE, Margrave JL, Hauge RH. *J Phys Chem B* 2001;105:1157.
- [25] Wu XB, Chen P, Lin J, Tan KL. *Int J Hydrogen Energy* 2000;25:261.
- [26] Darkrim FL, Malbrunot P, Tartaglia GP. *Int J Hydrogen Energy* 2002;27:193.
- [27] Schlapbach L, Züttel A, Gröning P, Gröning O, Aebi P. *Appl Phys A* 2001;72:245.
- [28] (a) Walter J, Shioyama H, Sawada Y. *Carbon* 1999;37:41; (b) Walter J, Shioyama H. *J Phys: Condens Matter* 1999;11:L21.
- [29] The amount of additional adsorbed hydrogen appears independent of the position (random or fixed) of atomic particles within

- the given network. (Guay P. M.Sc. Thesis, 2003, INRS-ÉMT, Varennes, Canada).
- [31] Alefeld G, Volkl J, editors. Hydrogen in Metals, vol. 1–2. Berlin: Springer-Verlag; 1978.
- [32] IEA/DOE/SNL On-Line Hydride Databases, <http://hydropark.ca.sandia.gov>.
- [33] Żaluska A, Żaluski L, Ström-Olsen JO. Appl Phys A 2001;72: 157.